Arab J Geosci (2016) 9: 182
DOI 10.1007/s12517-015-2206-8

ORIGINAL PAPER

Investigation and monitoring on a rainfall-induced deep-seated landslide

Momo Zhi[1] · **Yuequan Shang**[1] · **Yu Zhao**[1] · **Qing Lü**[1] · **Hongyue Sun**[2]

Received: 8 July 2014 / Accepted: 6 November 2015 / Published online: 3 March 2016

Abstract The ground movement of Xiashan village landside of Zhejiang province, China, commenced in 1958 due to typhoon rainstorms followed by two subsequent slips in 1989 and 2001. The reactivation of the large-scale landslide has become a serious concern to the safety of a nearby reservoir and the local villagers. A pilot testing program was established in 2007 using a variety of landslide monitoring facilities. The slope is of a chair-shaped form with Quaternary residual soil overlying the Pliocene sedimentary and basalt layers. The pilot test program included GPS, inclinometers of conventional and fixed types, piezometer, and rain gauge. Two potential sliding planes were identified in the inclinometers showing the possible slip mode along more than one bedding plane. A shallow slip surface dipping a low angle (10°) lies in the residual soil, while a deep slip surface is located along the weak plane within the Pliocene strata. The piezometer reading indicated high groundwater level and a certain level of correlation with the displacement velocity. A critical groundwater depth was determined, and its usage as a warning threshold was discussed. In view of the very important location about an existing dam, it is strongly recommended that surface and internal drainage facilities be provided to ensure the long-term stability of the landslide.

Keywords Landslide · Rainfall · Monitoring · Groundwater

✉ Yu Zhao
zhao_yu@zju.edu.cn

[1] Department of Civil Engineering, Zhejiang University, Hangzhou 310058, China

[2] Department of Ocean Engineering, Zhejiang University, Hangzhou 310058, China

Introduction

The rainfall-induced landslides occur every year in almost all mountainous areas throughout the world. Zhejiang province located in the southeast of China is prone to rainfall-induced landslides. There were more than 240 landslides occurred in Zhejiang territory which caused five casualties, six injuries, and more than 40 million RMB economical loss in 2014. Clear understanding of triggering mechanism and proper warning systems is of great significance for disaster mitigation especially for the mitigation of catastrophic landslides.

Seasonal intense rainfalls are recognized to be a primary triggering factor causing slope instability in sub-tropical regions (Tsaparas et al. 2003; Ng and Menzies 2007; Li et al. 2011; Leung and Ng 2013). The cause-effect relation has been studied and verified through detailed field investigation, field monitoring, numerical calculation, etc. Slope failures were related to groundwater conditions such as rainfall infiltration, antecedent moisture, and rainfall history (Wieczorek 1996). Wilson (1989) suggested that the buildup of water pressure in slopes caused by rainfall was the trigger of landslide.

Recently, the studies on rainfall thresholds for the initiation of landslides can classify the methods into two main directions, physical-based models and empirical models (Guzzetti et al. 2007). For physical-based models, various approaches had been proposed to predict the accumulation of infiltrated water into ground. The "leaky barrel" model proposed by Wilson (1989) considered the ground water system as a leaky barrel that received water from above at a given rate and lost water from below at a different rate. The accumulation of water was controlled by the recharge and leakage process, and the buildup of pore water pressure may cause slope failure. Cho (2009) proposed a one-dimensional infiltration model that extended Moore's infiltration model (Moore, 1981). It was used to evaluate the potential of a shallow slope

failure subjected to a particular rainfall event in account of the rainfall intensity and the duration in two-layered soil. For empirical models, Iovine et al. (2009) proposed an empirical approach of risk management on the basis of detailed geomorphologic field survey and the analysis of hydrologic data and superficial displacements. Then the criteria of the early-warning system was refined using limit equilibrium analyses based on real-time monitoring data collected from inclinometers and piezometers (Iovine et al. 2010).

The physical process models required detailed information such as hydrological, lithological, morphological, and soil characteristics (Guzzetti et al. 2007). Study concerning rainfall infiltration mechanism and its influences on stability of unsaturated soil slopes had been investigated through field monitoring programs (Smethurst et al. 2006; Liang et al. 2007; Tu et al. 2009; Pagano et al. 2010). The empirical models needed more monitoring data such as precipitation amount, duration, and intensity of rainfall, displacement, and groundwater level of the landslides. According to Iovine et al. (2010), real-time data acquisition via GSM was appropriate when cable-based transmissions were impracticable.

For the shallow landslides or soil slips (Cruden and Varnes 1996), the occurrence may be attributed to rainfall infiltration and directly connected with the amount of rainfall (Ma et al. 2015). However, the mechanism of large-scale landslides was usually more complicated and varies from case to case (Doglioni et al. 2012). In the present paper, the detailed information of Xiashan village landside of Zhejiang province, China, was first collected via geological investigation. Basic features and triggering factors were determined combing the historical records of the landslide activation and crude statistic of rainfalls. A pilot testing program with a variety of monitoring facilities program was established in 2007 and operated in order to study the mechanism and get a better warning criterion for the landslide. We are expecting that the new working approach can to some extent reduce the effort needed for the emergency management for rainfall-induced large-scale landslides.

Study area

General description

Zhejiang province is located in Southeast China in a subtropical region, and 70.4 % of the province is mountainous or hilly. There were more than 4200 landslide hazards and potential hazard points in the province (NBS 2011). Many landslides were induced owing to seasonal rainfall and torrential rain caused by Typhoon.

Xiashan village landside was about 8.25 million m^3 with an affected area of almost 252,000 m^2. This biggest rainfall-induced landslide in Zhejiang province shows slowly and uninterruptedly sliding at present. It is located approximately 250 m to the east of Shimen Reservoir and minimum 152 m above it (Fig. 1). The complete instability of the slide mass will probably generate a potentially destructive seiche in the reservoir, which is a huge threat to the local villagers. Unfortunately, the movements were not recorded in detail before 1958. There were two obvious sliding since 1958. The slope mass moved to west suddenly after the typhoon rainstorm on July 30th, 1989, and slid again several days after the heavy rain on July 6th, 2001.

The landslide is kidney-shaped (Figs. 1 and 2a) in the plane view. The slide mass is 1120 m wide (in the north-south direction) and 290 m long. The trailing edge appears like a huge round-backed armchair. The elevation of the landslide head is 356–410 m, while the elevation of the toe is 302–354 m. The

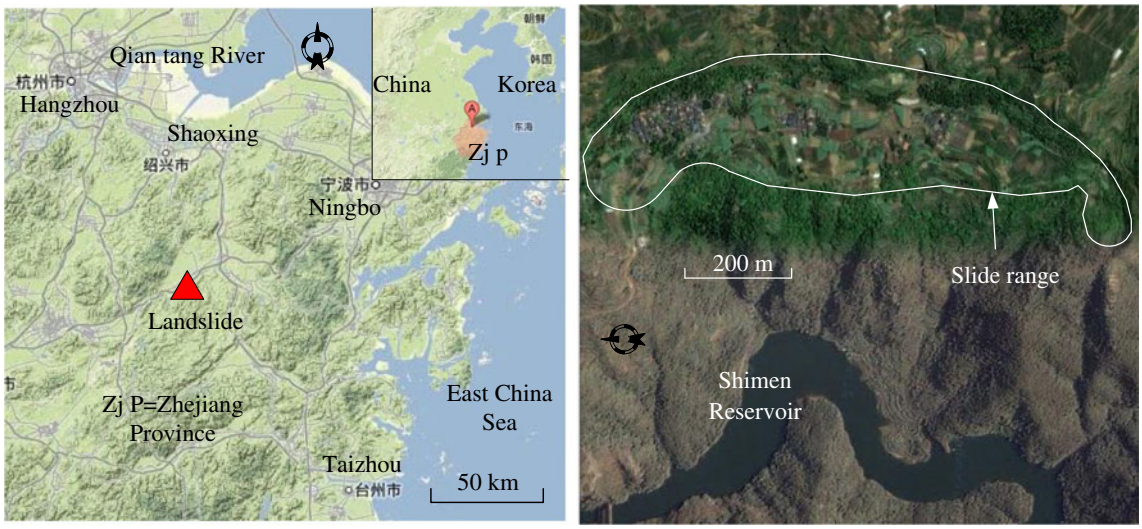

Fig. 1 The location of the study area (the satellite image is obtained from Google map)

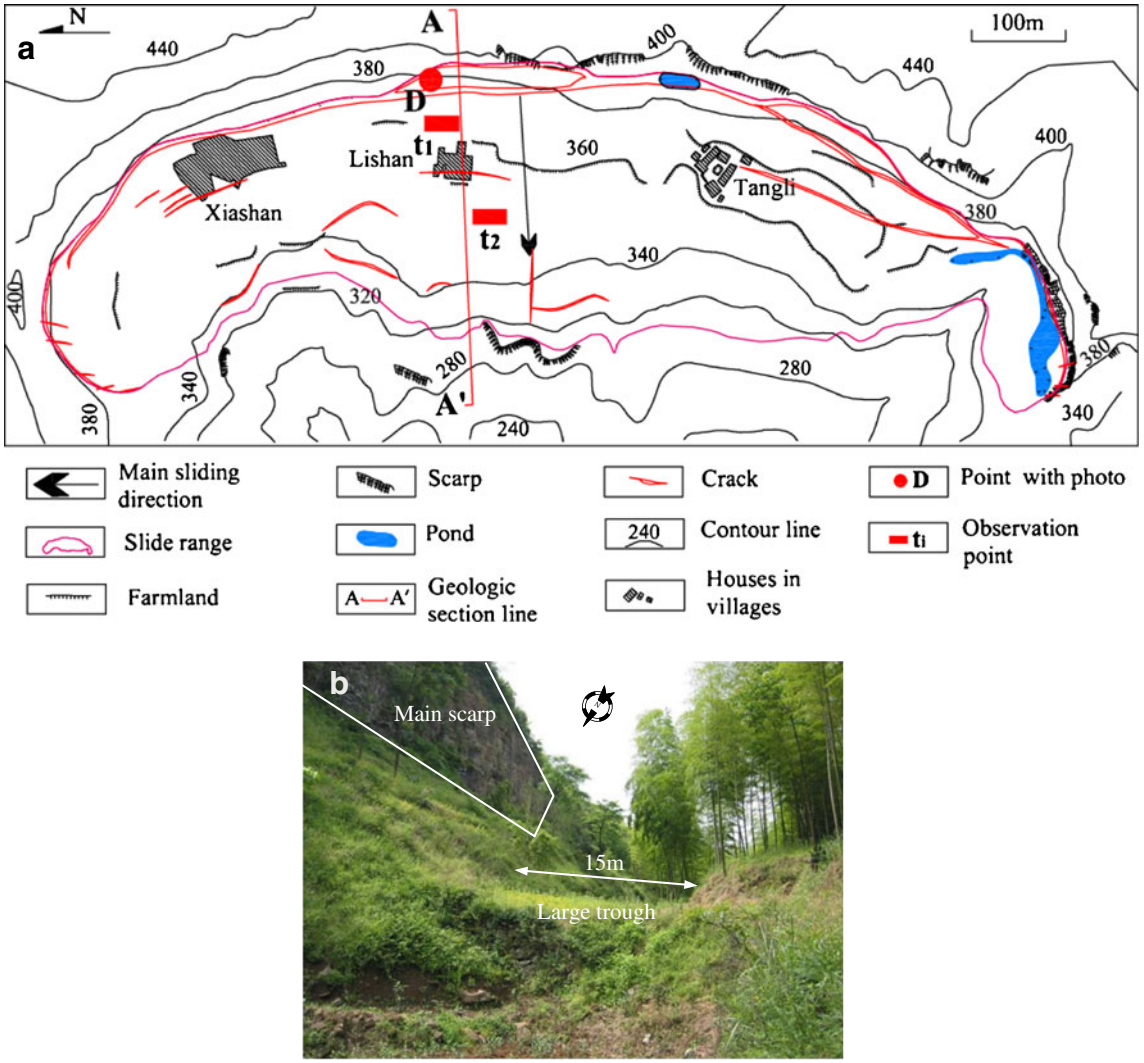

Fig. 2 Geomorphological features of the Xiashan village landslide, **a** plane view and **b** photo of the large trough and main scarp (photo taken at *D* point)

toe of the landslide is in wave shape. The sliding direction is terrain-dependent, and the main direction is 265° near the geological profile A-A'.

Twenty-four representative cracks were recorded from field observation as shown in Fig. 2a, and a photo of the main scrap is shown in Fig. 2b. Tension cracks were 100–300 m long and 0.5–3 m wide and mainly distributed in the rear of the landslide mass. Bulge cracks with the size of 50–150 m in length and 0.3–2 m in width were generated in the middle and the front portion of the slide mass. Radial cracks were mainly distributed in the toe of the landslide. There were also few shear cracks distributing in the south and north part of the landslide mass. We can see large trough in the rear of the landslide, one (length 50 m, width 15 m) of which was in the middle of the slide mass with many plants grow in as shown in Fig. 2b.

During June 2004 to August 2006, the Institute of Disaster Prevention Engineering of Zhejiang University monitored the landslide and obtained the displacement, groundwater level, and rainfall data. The construction of a pilot monitoring program started in July 2007 and completed in June 2013 in the landslide area, and about 700 indigenous villagers who lived in three villages (Fig. 2a, Xiashan, Lishan, and Tangli) in the area were resettled in a town nearby. A monitoring system with solar-powered and wireless transmission then came into operation and started to transmit real-time monitoring data back to the authors' laboratory in high frequency.

Local geology

Discontinuities such as joints developed in the rock masses in the area due to regional tectonic movements. There are four regional tectonic belts in the area (three of them are in NE direction and one in EW direction), which made original vertical joints in basalt stretch further.

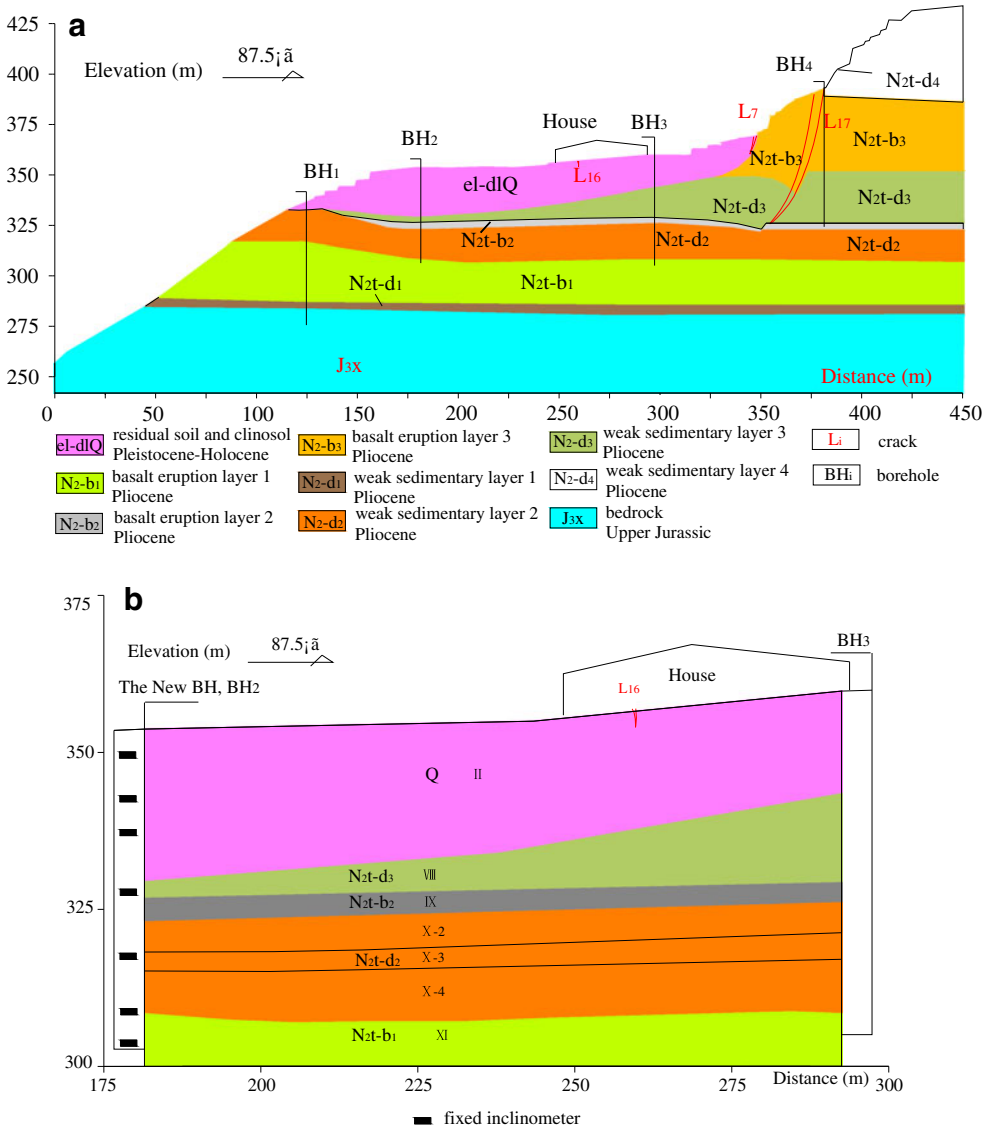

Fig. 3 Geological profile along the section A-A' **a** the entire view and **b** profile between boreholes 2 and 3 with the location of the new borehole and fixed inclinometers (soil property, aquosity, and penetrability of the layers are shown in Table 1)

Figure 3a presents the geological profile A-A' of the slope obtained from four boreholes and the cut face exposures. The slope mainly consists of three strata, including the Upper Jurassic Xishantou Formation (J_3x), the Pliocene Chengxian Group Tonglingzhu Formation (N_2t), and the Quaternary residual soil and Holocene clinosol (Q).

The J_3x layer was mainly composed of intact tuff, tuffaceous sandstone, and tuffaceous glutenite. The bedrocks of this layer had very rare joints and cracks. The sedimentary and basalt eruption stratum N_2t that has an unconformity contact with the underlying J_3x layer can be further divided into five layers, $N_2t\text{-}d_1$ ~ $N_2t\text{-}b_5$. The Q layer contained residual soil (el-dlQ, silty clay with angular gravel and gravelly soil with silty clay) and Holocene clinosol (dlQ_4, gravelly soil with silty clay). The landslide formed a sequence of permeable and impermeable layers inside as shown in Fig. 3b and Table 1.

Climate

The rainy season of the sub-tropical monsoon climate in this area consists of spring rain (end of March to begin of June), plum rain (mid-June to mid-July) and typhoon rainstorm (late July to September). The average annual precipitation is approximately 1497.4 mm during the period 1965–2002. The rainfalls could reach 679.4–1638.8 mm during the rainy seasons, and 55–65 % of the rainfalls was concentrated between May and August. The maximum span of plum rain period lasted 23 days, and the quantity of precipitation was up to 476.3 mm. The yearly peak value of seven consecutive days was about 91–321.2 mm (179.7 mm in average).

It is obvious that the historical sliding was closely related to rainfall. The quantity of precipitation reached 188.6 mm in the last 10 days before the landslide slid on July 30th, 1989. The reactivation occurred again several days after a heavy rain

Table 1 Soil property, aquosity, and penetrability of the layers between borehole 2 and borehole 3

Stratum		Soil property	Aquosity	Penetrability
el-dlQ	II	Gravelly soil with silty clay	Seasonal aquifer	Permeable
N_2t-d_3	VII	(Peaty) clay with sand interlayer	Aquitard	Impermeable
N_2t-b_2	IX	Highly weathered basalt		
N_2t-d_2	X-2	Clay, partly soft plastic		
	X-3	Sandy gravel	Main aquifer	Permeable
	X-4	Hard plastic sandy mudstone and clay	Aquitard	Impermeable
N_2t-b_1	XI	Moderately weathered basalt	Aquifer	Permeable

(maximum daily value reached 41.5 mm and cumulated rainfalls over 7 days were up to 132.4 mm) on July 6th, 2001.

Hydrology

There were two types of groundwater in the landslide area, water in the residual soil and water in rock fissures. The groundwater in the residual soil had obvious seasonal feature. The fissure water existed in sandy gravel layer of Pliocene Chengxian Group Tonglingzhu Formation (N_2t) and the intermediary weathered basaltic rock. The sandy gravel layer X-3 (Fig. 3b) was the main aquifer, and the overlying and underlying strata were relatively impermeable, which makes phreatic groundwater tend to become artesian groundwater. Rainfall recharge was the main supply to groundwater. Twenty springs and three wells were recorded in the landslide area during the field investigation, and the amount of their discharge was about 4.60–4.70 L/s. The total discharge in the area could increase to 8.2 L/s during the rainy season.

Field measurements

The landslide was monitored by the authors' institute during June 2004–August 2006. The authors also started to obtain other data in addition to deep displacement including the surface displacement, rainfall, and groundwater variation since March 2012 using the solar-powered fully automated system. The system was able to send real-time data back to the monitoring center wirelessly as shown in Fig. 4. The specification of the instrumentation is listed in Table 2. The observational data together with the collected climate and precipitation data (1976–2013) were reviewed in order to discuss the triggering mechanism of the landslide.

Deep displacement

The deep displacement from July 10th, 2004, to January 30th, 2005, along borehole 1 illustrates the sliding trend along the main sliding direction of the landslide as shown in Fig. 5a. The displacement curve illustrated the sliding trend along the main sliding direction of the landslide, and the maximum deformation reached 12.2 mm at the top of the borehole. The deformation occurred during two periods, one from July 10th, 2004, to September 12th, 2004 (the cumulative displacement was about 3 mm) and the other one from December 3rd, 2004, to January 30th, 2005 (the cumulative displacement was about 8 mm). Two main inflection points corresponding to the two sliding zones, the one between 3.0 and 8.0 m and the other between 14.0 and 20.0 m, were observed from Fig. 5a.

During the construction of the wireless solar-powered monitoring system, we drilled a new borehole (at point t_2, 50.8 m deep) near borehole 2 and installed seven fixed clinometers in it (Fig. 3b) in order to monitor the deep displacement of the landslide. The fixed clinometers could send monitoring data back to the laboratory once every 4 h. The deformation curves from March 2012 to September 2013 of the monitored points at different depth are illustrated in Fig. 5b, c.

Figure 5b illustrates the cumulative deep displacement along the new borehole at point t_2 monitored with the fixed inclinometer. It is noted in Fig. 5b, c that the displacement accumulated in 1 year at 26.0, 36.0, 45.0, and 50.0 m deep was less than 1 mm, which indicates that the landslide did not slide along the deep slip surface. In comparison, larger displacement at 4.2, 11, and 16.2 m indicates that the displacement focused on the shallow slip.

Groundwater level and rainfall

The groundwater level observed in borehole 3 and the daily rainfall in the landslide area from July 2004 to February 2005 is shown in Fig. 6. The depth of groundwater level fluctuated in the range of 10.48 ~ 17.9 m during the monitoring period. The groundwater depth uplifted to 11.40 m after the rainstorm on August 13th, 2004 (daily precipitation 141 mm), which

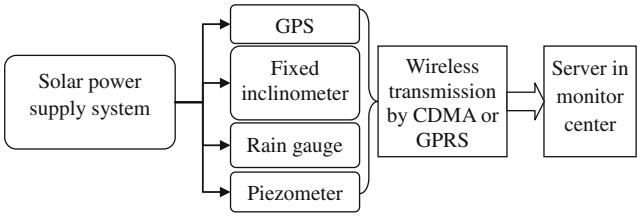

Fig. 4 Schematic diagram of the monitoring system

Table 2 Specification of instrumentation

Instrument	Brand and model	Specification
GPS	Huace Corp. X60M dual frequency receiver	L1 and L2 carrier phase measurement at 5 Hz update rate, precision better than 1 mm
Piezometer	Geokon Corp. BGK-4500AL	Range 0 ~ 70 kPa; resolution 0.025 % FS; precision 0.1 % FS (full scale); overload capacity 2 × FS
Fixed inclinometer	Geokon Corp. BGK-6150MEMS	Range ±15°; resolution ±10″ (±0.06 mm/m); precision 0.1 % FS
Conventional inclinometer	China Aerospace Science and Industry Corp. CX-01	Resolution 0.02 mm/8″; precision ±4 mm/15 m
Rain gauge	Newall Measurement Systems Corp. tilting rain gauge	Range 0 ~ 6 mm/min; resolution 0.1 mm; $\begin{cases}\delta \le \pm 0.2, p < 10\\ \delta \le \pm (0.2 + 1\ \%\ \mathrm{FS}), p \ge 10\end{cases}$

p precipitation mm

was owing to the gathering and infiltrating of rainfall in the rear of the landslide. The groundwater showed obvious rise on October 16th and December 22nd, 2004, when there was no rainfall before the rise. The groundwater depth uplifted from 14.0 to 10.48 m on December 8th, 2004, but the antecedent precipitation was only 30.2 mm, and thus the groundwater was mostly influenced by some other factors. Before the government relocated the original inhabitants in June 2007, they planted tea and other crops on the terraces distributed in the rear of the landslide. The local residents introduced a new tea variety from late November to early December 2004 and irrigated the area several times in order to keep the proper moisture content of the soil during the tea planting, which caused a significant rise of the groundwater in borehole 3.

After the resettlement of the local residents, the influence of human activity on groundwater level was reduced dramatically. The amount of the rainfall in the landslide area and groundwater level of point t_1 was then obtained through the real-time monitoring system. The groundwater level of point t_1 and the daily rainfall in the landslide area from April 2012 to May

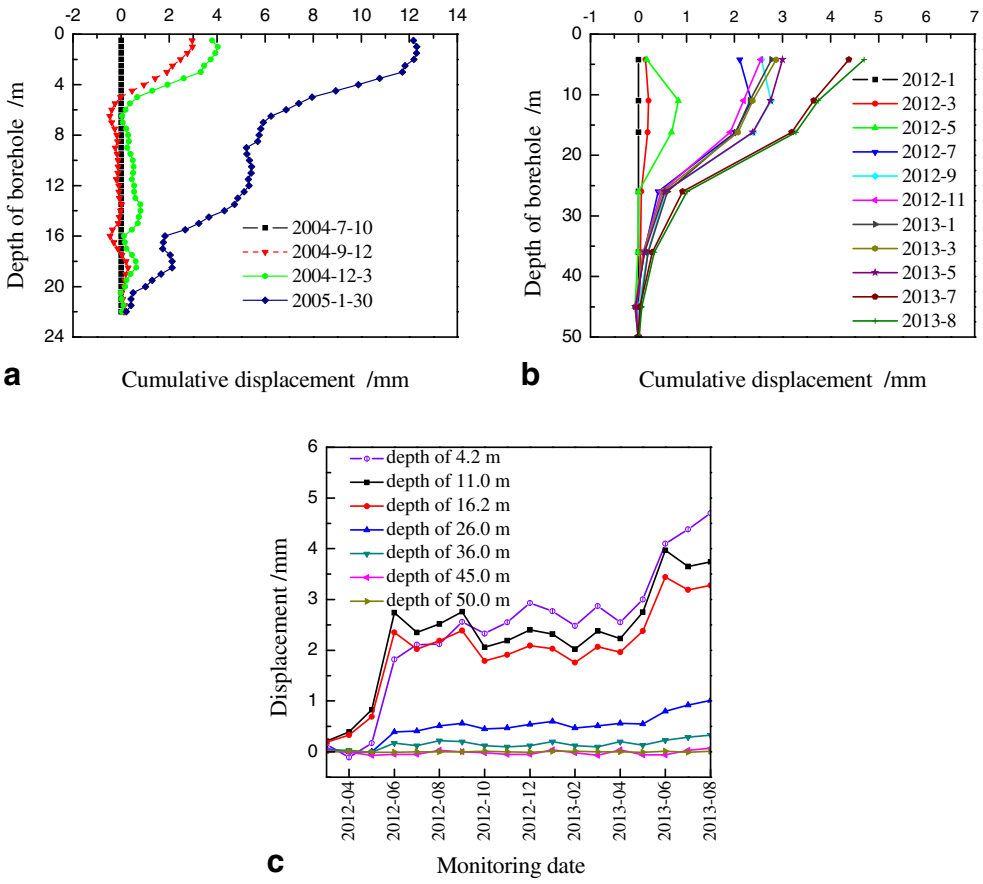

Fig. 5 Cumulative deep displacement curve of conventional inclinometer and fixed inclinometers, **a** displacement at borehole 1, **b** displacement at the new borehole, and **c** displacement in different depth at the new borehole

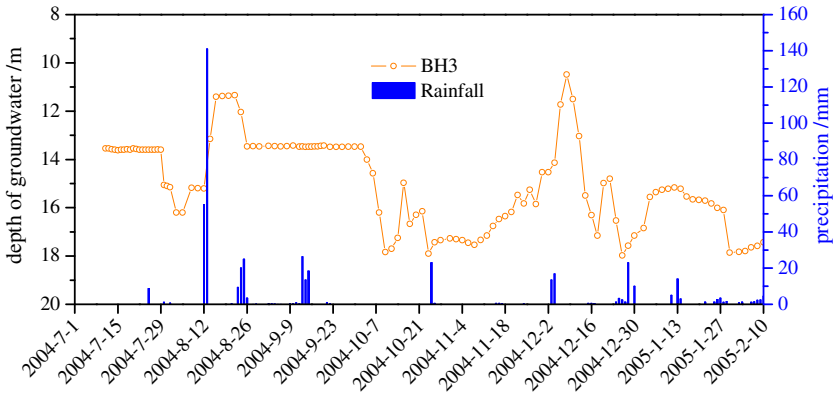

Fig. 6 Daily rainfall in the landslide area and groundwater depth in borehole 3 monitored from July 2004 to February 2005

2012 is shown in Fig. 7, exhibiting positive correlation between them.

The groundwater level of the borehole at point t_1 changed along with the rainfall intensity and duration. The groundwater level rose rapidly when the amount of rainfall was large and could maintain a relative high level for a long period when the rain lasted for several days. Although the rainfall and the rise of the groundwater had a cause-effect relationship, obvious hysteresis existed between them. The lag phase probably depended on the amount of rainfall. The phase was very short when the amount of rainfall reached 30 mm during the observation period, because the rainfall input was far beyond the discharge capacity of the landslide groundwater system. The lag could be about 2 or 3 days when the rainfall was subtle.

Surface displacement

We collected the surface displacement of point t_2 along the geological profile A-A' using a GPS monitoring system. GPS dual frequency receiver was used at the monitoring station in order to improve the precision of measurement. The monitoring system could eliminate background noises automatically and resolve the displacement data of station t_2 per hour with a measuring accuracy better than 1 mm.

The monitored data of station t_2 from March 2012 to September 2013 is illustrated in Fig. 8. The landslide was sliding at a very low deformation rate, which indicated that the landslide was in a creep state between stable and unstable. The accumulated displacement during the 1.5 years was approximately 5 mm as shown in Fig. 8. The selected monitoring period contained two rainy seasons and a dry season, and the histogram of monthly precipitation indicated the concentration of rainfall during the rainy season. The surface displacement appeared intermittent and periodic. The deformation was concentrated during the rainy season (April 2012 to July 2012 and April 2013 to August 2013) and the landslide was relatively quiescent in dry season. Simultaneously, the displacement was closely related to the precipitation by comparing the curves in Fig. 8.

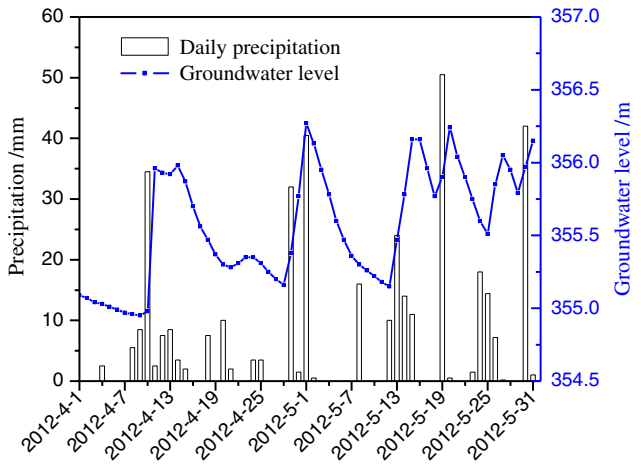

Fig. 7 Daily precipitation in the landslide area and groundwater level of point t_1 (April–May 2012)

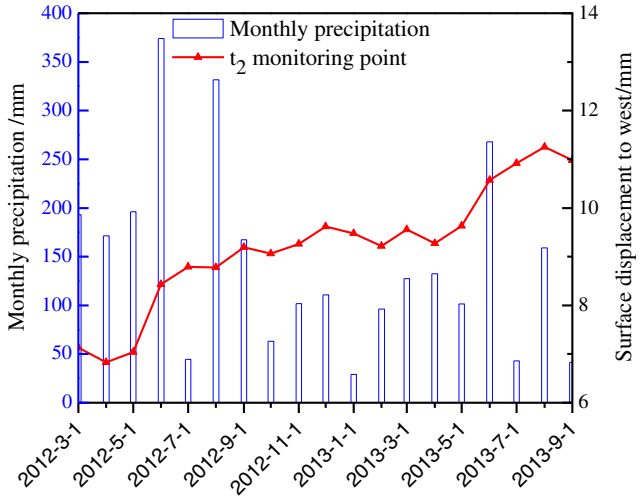

Fig. 8 Monthly precipitation in the landslide area versus surface displacement curve of t_2 monitored by GPS

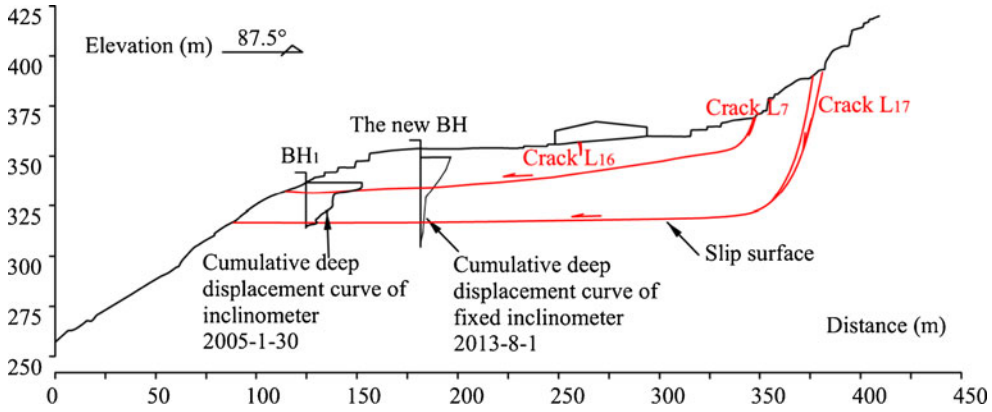

Fig. 9 Profile of Xiashan village landslide: inclinometer and fixed inclinometer measure and slip surfaces

Landslide features and mechanism

Landslide features

Combining the two sliding zones determined by the deep displacement, the cores from the boreholes, and major tension cracks, we could depict two main slip surfaces as indicated by the red solid line in Fig. 9. The cores at the depth of the slip surface showed obviously compressional and kneaded features, where the soil had obvious plastic deformation and the gravel was polished. The shallower slip surface dipping very low angle (10°) lays in the residual soil, while the other was along weak layer within the Pliocene strata. For the deeper one, the back part was very steep (60°–80°) and the middle and front parts were rather flat or even slightly depressed. In concern of geomorphologic characteristics of the area and the shape of the slip surfaces, the mode of sliding was confirmed as compound slide according to the classification proposed by Cruden and Varnes (1996). The landslide deformed continuously and the velocity varied in different periods. Cumulative deep displacement monitored in 2004 and 2012 indicated that the velocity was less than 16 mm/year, and thus the landslide may be characterized as an "extremely slow" class. The maximum observed displacement at the toe of the landslide was approximately 2000 mm on July 30th, 1989, and the corresponding velocity 2.0 m/year can be classified into a "slow" class.

The deep displacement monitored from March 2012 to September 2013 shows that the major deformation concentrated on slope mass above the shallow slip surface, whereas the deformation of the deeper portion was little. Comparing this slipping trend with the two previous records of obvious sliding indicated that the deep portion of the landslide mass was in a stable state in normal rainy season and the shallow slip surface was active at a low deformation rate. The landslide might slip along the deep slip surface again when the rain is extremely heavy and long-lasting, and the shallow deformation rate might become high at the same time.

Landslide mechanism

The geomorphological and geological features rendered the slope mass vulnerable to rainfall. The landslide had a stair-shaped profile and the trough in the rear of the landslide made the surface water gather quickly. The groundwater can infiltrate deeply into the landslide easily due to various cracks and vertical joints and fissures along the slip direction. The front edge of the landslide mass

Table 3 Monthly rainfall amount obtained from Huishan town hydrological station (2.3 km from the site)

	Jan	Feb	Mar	Apr	May	Jun	Jul	Aug	Sep	Oct	Nov	Dec	year
Average (1976–2013)	72.7	80.5	135.4	132.3	139.0	227.7	149.8	217.6	146.7	68.3	69.1	53.3	1492.5
1989	94.1[a]	68.5	82.7	159.8[a]	200.6[a]	309.1[a]	331.8[b]	221.8[a]	340.5[a]	23.7	28.4	74.0[a]	1935.0
2001	116.5[a]	90.5[a]	95.9	56.0	109.9	323.1[b]	83.1	184.7	69.4	19.6	105.5[a]	103.8[a]	1296.4
2004	68.3	68.8	53.9	51.8	197.3[a]	25.2	148.5[a]	254.3[b]	140.6	24.3	49.6	139.0[b]	1221.6
2005	91.8[a]	169.1[a]	98.6	84.3	151.7[a]	54.7	198.7[a]	234.3[a]	186.3[a]	67.6	70.9[a]	61.8[a]	1469.8
2012	135.7[a]	82.8	193.0[a]	171.5[a]	196.0[a]	374.0[b]	44.5	331.5[b]	167.5[a]	63.0	101.8[a]	110.6[a]	1971.9
2013	29.2	96.2[a]	127.5[a]	132.5[a]	101.5	268.0[a]	43.0	159.0	41.5	271.0[a]	32.5	112.0[a]	1413.9

[a] Values greater than monthly average

[b] Months that cover the sliding events

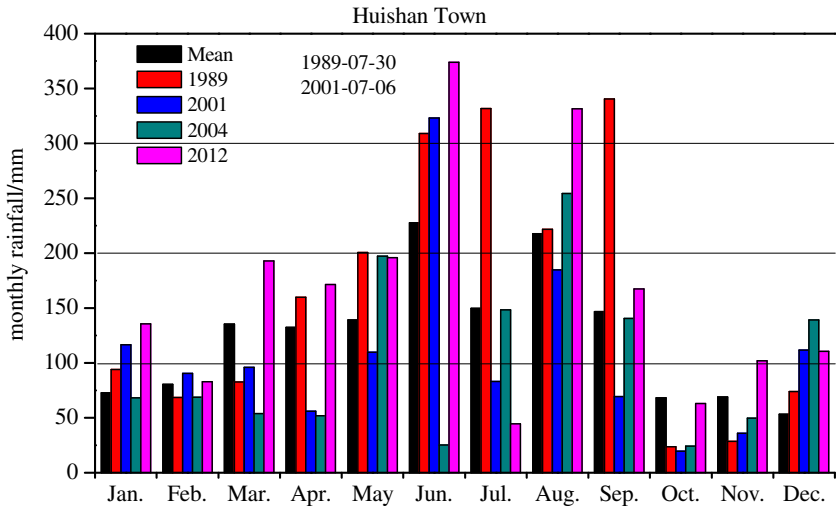

Fig. 10 Rains recorded during the 1989, 2001, 2004, and 2012 hydrological years compared to monthly rainfalls

was steep cliff and steep slope, which was propitious to the development of the deformation and failure. The loose Quaternary residual soil could be easily saturated and tend to produce plastic deformation under the action of water. In addition, the weak sedimentary layer of Pliocene Chengxian Group is prone to compaction and deformation owing to groundwater.

We collected annual rainfall data between 1965 and 1975 and monthly data afterwards from Huishan town hydrological station. Statistics of monthly rainfall from 1976 to 2013 are shown in Table 3. Rainfall mainly concentrated during the rainy seasons between March and September, and the records of sliding also indicated deformation occurred mainly in June, July, and August. However, the deformation recorded in December 2004 (8.0 mm) was caused by the uplifting of the groundwater owing to the irrigation during the tea planting.

In addition, the special strata sequence of impermeable and permeable layers of the landslide make the phreatic groundwater tend to become artesian groundwater (Hodge and Freeze 1977; Rogers and Selby 1980). Largely varying permeability of soil layers is another important factor for slope stability (Terzaghi and Peck 1967; Deere and Patton 1971; Jiao and Nandy 2001; Jiao et al. 2005). The deep slip surface was along the second sedimentary layer of the Pliocene Chengxian Group Tonglingzhu Formation ($N_2t\text{-}d_2$, X-2, and X-3). The X-2 and X-4 layers consisted of impermeable river or lacustrine deposition clay, while the X-3 layer was permeable sandy gravel. The permeability differences made it possible that the phreatic groundwater became artesian groundwater especially when permeable layer was blocked at the toe of the landslide, and the landslide may became unstable due to the high water pressure. A similar mechanism was also evidenced in another case history of the same province (Sun et al. 2013; Zhao et al. 2012).

Discussions

The most noticeable sliding in record occurred in 1989 with approximately 2000 mm displacement at the slope toe, while the displacement was about 60–100 mm in 2001. Deep deformation monitored with inclinometer indicated the cumulative displacement was less than 15 mm in 2004 and 2012. Monthly rainfalls during the activation of the landslide (1989, 2001, 2004, 2012) were all greater than average values as shown in Fig. 10 and Table 3. It seems that the movement of the slope mass was closely related to the amount of rainfall. However, the variation of cumulated rainfalls over 30–60–90–120 days in Fig. 11 illustrated that the cumulated rainfalls in 2001 and 2004 were much less than that in 1989 and 2012, whereas the displacement in 2001 was remarkably greater than that in 2012. The variation of groundwater depth in borehole 3 and amount of rainfall was monitored from July 2004 to February 2005 (Fig. 6), and the obvious rise of the groundwater (August 10th, October 16th, and December 22nd) was owing to irrigation of in the rear of the landslide (personal communication with local inhabitants). The government relocated the original inhabitants to Huishan town since June 2007 before the construction of the pilot test program, and afterwards, the groundwater level was no longer influenced by irrigation. Since the rainfalls in 1989 were extremely rich, the influence of irrigation activity can be ignored.

As shown in Fig. 12a, maximum rainfalls cumulated over 30, 60, 90, and 120 days in 1989, 2001, 2004, and 2012 are compared with the historical maxima in 1976–2013. Historical maximum rainfalls cumulated over 30, 60, 90, and 120 days occurred in 1990, 1987, 1992, and 1989, respectively, and annual maximum rainfalls occurred in 2012. It is not reasonable to attribute the reactivations in 2001 and 2004 to rainfalls if we consider the very low position of the two curves in Fig. 12a. The 1989 curve is the highest among the four and the 2012 curve lies below almost in parallel. The 30-

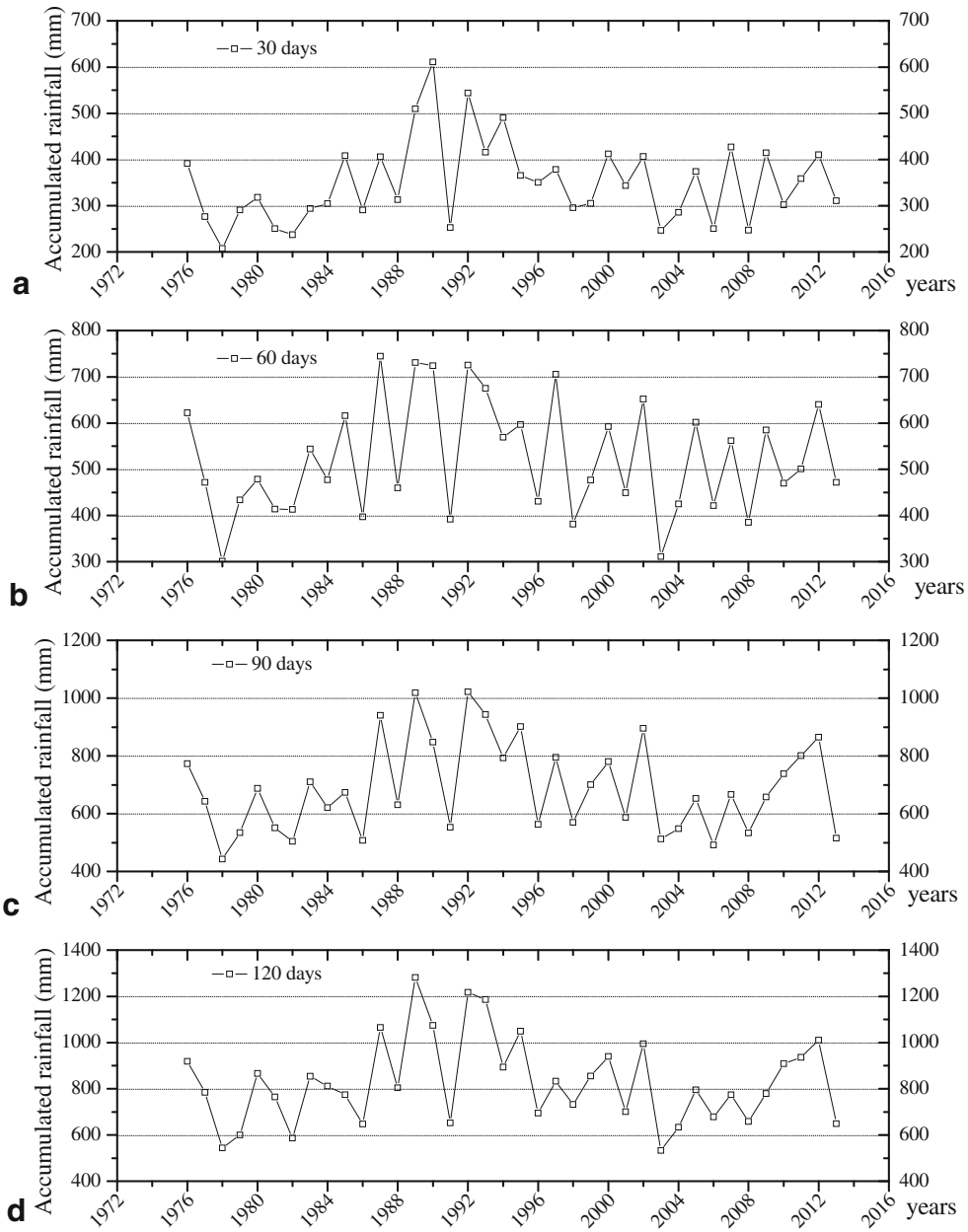

Fig. 11 Rainfalls cumulated over **a** 30, **b** 60, **c** 90, and **d** 120 days during the period 1976–2013

day rainfall in 1989 was slightly lower than the historical maximum, while the records over 60, 90, and 120 days in 1989 almost coincided with historical maxima. Iovine et al. (2010) also discovered that a high cumulative rainfall curve might be connected with a reactivation. If we take the 1989 curve as a higher bound and 2012 curve as a lower bound, a rainfall curve that lies in between will probably cause a sliding event.

However, the amount of displacement or even the reactivation was not always correlated with the amount of rainfalls. The five peaks in Fig. 11 indicate the abundance of rainfall in 1987, 1989, 1990, 1992, and 2012, and Fig. 12b shows the monthly rainfalls of the five years. No large deformation was evidenced or recorded in 1987 whose monthly rainfall curve is very similar to that of 1989. The 1990 and 1992 curves have similar trend with the 2012 curve, but no obvious sign of deformation was observed in either of the two years. The phenomenon was also observed in the case of Petacciato landslide in Italy (Doglioni et al. 2012). The cumulative rainfalls of several reactivations were less than the average value.

It is noticeable that the landslide was not reactivated in September 1989 after the dramatic sliding, given that the monthly rainfall was 2.3 times the average. Due to the evolution of infiltration and discharge conditions during the sliding process, groundwater variation might response differently to the same or similar condition of rainfalls. Since the buildup of water pressure into ground caused by rainfall is the trigger of

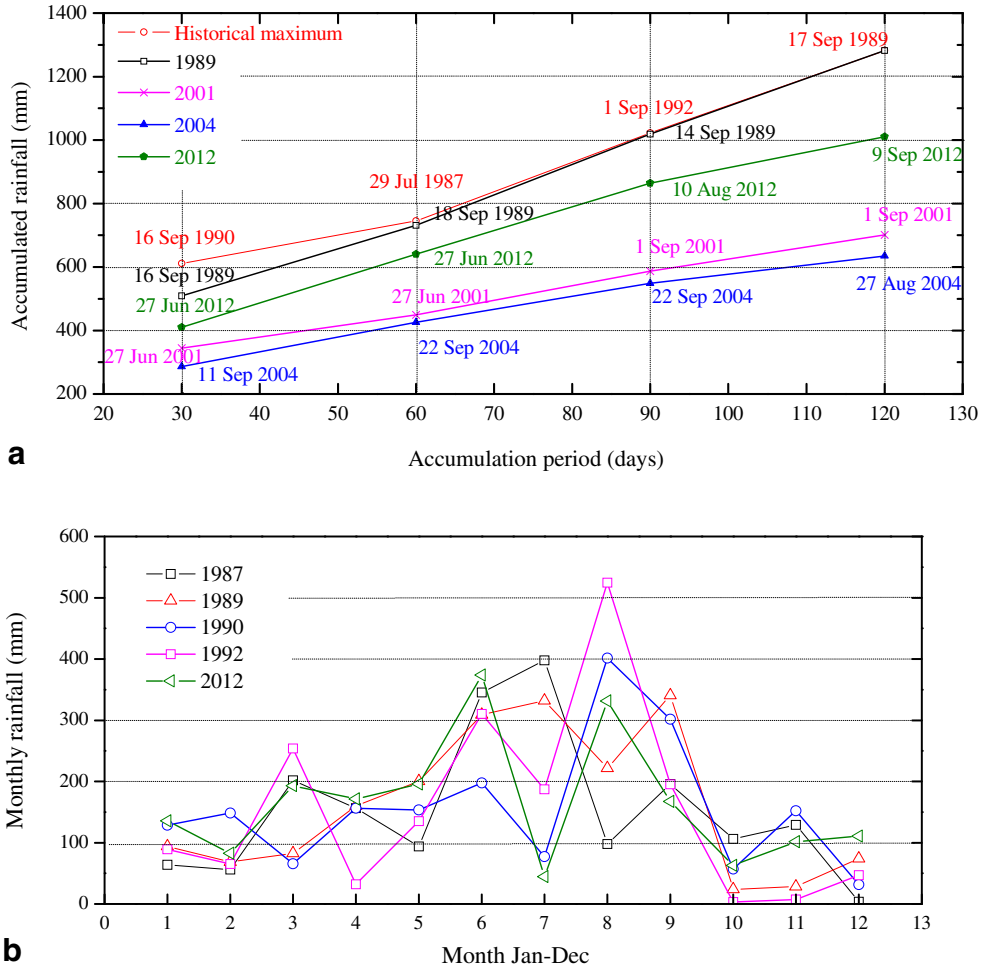

Fig. 12 **a** Rains recorded during the 1989, 2001, 2004, and 2012 hydrological years, compared to historical maxima (period 1976–2013) in terms of accumulated rains, and **b** monthly rainfalls during the years when the historical maxima accumulated rains occurred

landslide (Wilson 1989), the deformation of the landslide may be more sensitive to groundwater level than rainfalls.

The groundwater, rainfalls, and displacement of the landslide were frequently monitored during the period of 2012–2013. The surface displacement curve in Fig. 8 exhibits two notable segments of increase during the rainy seasons from May to August in 2012 and 2013, respectively. Considering that the water level in the slope was more directly connected with the slope movement, the surface displacement and the depth of water level between April and August in 2012 were re-plotted with denser data in Fig. 13 to check the correlation in detail. Five obvious water level peaks, PL1~ PL5 are observed, and the first three and the last two correspond to the two segments of displacement increase in June and August, respectively.

The displacement velocity was also calculated and plotted with the depth of water level in Fig. 14. Although the groundwater level was sensitive to rainfall events and varied

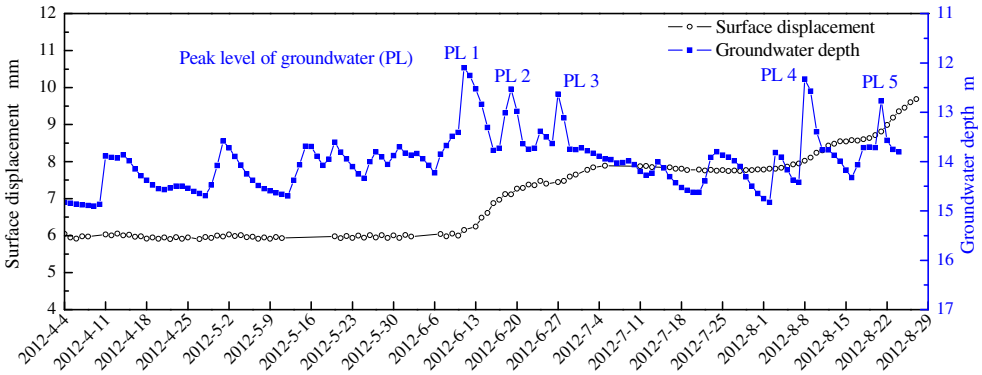

Fig. 13 Surface displacement monitored at point t_2 by GPS and groundwater depth in the landslide area (from April 4th to August 28th, 2012)

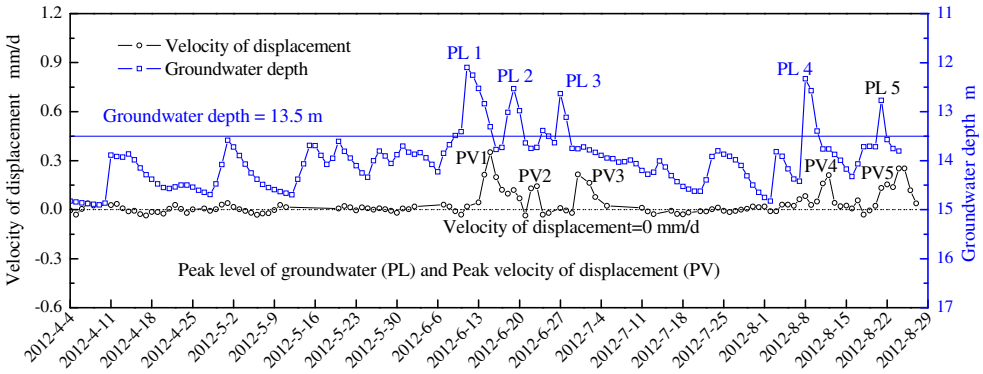

Fig. 14 Velocity of surface displacement at point t_2 by GPS and groundwater depth in the landslide area (from April 4th to August 28th, 2012)

frequently, the variation of displacement velocity was not always evident accordingly, e.g., the segment between April and early June of the velocity curve and the segment in mid-July are quite flat with merely negligible fluctuations when the groundwater depth was deeper than 13.5 m. However, five water level peaks PL1 ~ PL5 where the depth was shallower than 13.5 m induced five distinct peaks PV1 ~ PV5 on the velocity curve, respectively. The details of PVs and PLs are listed in Table 4. The velocity peaks varied between 0.16 and 0.35 mm/day and appeared approximately 80 h later than the peaks of groundwater level. It is indicated that 13.5 m is the critical groundwater depth in this case.

Once the correlation between the groundwater level and displacement velocity is established as shown in this case, solely, the monitoring of water level is needed for the early warning of the landslide. Compared with a sophisticated monitoring system and warning system (Iovine et al. 2010), the money spent on monitoring can be significantly reduced as the economic cost is closely related to the number of monitoring items. In addition, we still had sufficient time (80 h in this case) to take countermeasures when a water level warning was received, but displacement monitoring may not provide enough time.

In consideration of the importance of groundwater level to the stability of a slope, we should take measures to reduce the effect of groundwater, e.g., digging annular intercepting drain above the trough at the back edge of the landslide which could prevent the surface water from gathering and flowing into the landslide area quickly. Another possible measure is drilling seepage wells and drain holes or tunnels near the main aquifer in the landslide, increasing the drainage discharge of the groundwater. The engineering measures may limit the rising of the water level and the water pressure and finally improve the stability of the landslide.

Conclusion

Xiashan village landslide may be considered as a typical case of rainfall-induced landslide, which slid several times so far and deforms continuously. The investigation revealed two low-angle slip surfaces, the shallow one in the residual soil and the deep one along the weak plane within the Pliocene strata. Considering the geomorphologic characteristics and the shape of the slip surfaces, the mode of sliding was confirmed as a compound slide. According to the velocities in different periods, the landslide was in a "very slow" state most of the time and may occasionally develop into a "slow" class.

Before the resettlement of the local residents in June 2007, human activities such as irrigation had great influence on the groundwater level and the stability of the slope. It was still difficult to quantify the relationship between the amount of displacement and the amount of rainfalls with the limited data available. However, the velocity of surface displacement is more closely related to the groundwater level, and the groundwater depth of 13.5 m can serve as a warning threshold in this specific case. The time lag between the water level peak and velocity peak provided us sufficient time for countermeasures, which demonstrates the feasibility of a warning system with water level monitoring only. For a rainfall-induced deep-

Table 4 Statistical data of peak value of groundwater level (PL) and displacement velocity (PV) and the lag time between them

Peak value number	Monitor date (PL)	PL (depth m)	PV (mm/d)	Lag time (h)
1	June 11th	12	0.35	89
2	June 19th	12.54	0.16	87
3	June 27th	12.6	0.26	83
4	August 8th	12.2	0.22	81
5	August 21st	12.7	0.27	85

seated landslide, we need to figure out its mechanism through investigation and monitoring first, and then determine a proper groundwater level as the warning threshold. The study approach is worth considering for similar cases.

Acknowledgments The study is supported by the National "Twelfth Five-Year" Plan for Science & Technology Support (No. 2012BAK10B06), the National Natural Science Foundation of China projects (No.51208461 and No.41202216), and the Fundamental Research Funds for the Central Universities (No.2014QNA4016 and No.2014QNA4020).

References

Cho SE (2009) Infiltration analysis to evaluate the surficial stability of two-layered slopes considering rainfall characteristics. Eng Geol 105(1):32–43

Cruden DM, Varnes DJ (1996) Landslides types and processes, in: Landslides: investigation and mitigation, edited by: Turner, A. K. and Schuster, R. L., Transportation Research Board Special Report 247, National Academy Press, WA, 36–75.

Deere DU, Patton FD (1971) Slope stability in residual soils. Proc. 4th Panamerican Conf., Soil Mech. Puerto Rico, vol 1:87–170

Doglioni A, Fiorillo F, Guadagno FM, Simeone V (2012) Evolutionary polynomial regression to alert rainfall-triggered landslide reactivation. Landslides 9(1):53–62

Guzzetti F, Peruccacci S, Rossi M, Stark CP (2007) Rainfall thresholds for the initiation of landslides in central and southern Europe. Meteorog Atmos Phys 98(3–4):239–267

Hodge RA, Freeze RA (1977) Groundwater flow systems and slope stability. Can Geotech J 14:466–476

Iovine GGR, Iaquinta P, Terranova OG (2009) Emergency management of landslide risk during autumn-winter 2008/2009 in Calabria (Italy). The example of San Benedetto Ullano, In Proceedings of 18th World IMACS Congress and MODSIM09 Int. Congress on Modelling and Simulation: 2686–2693.

Iovine GGR, Lollino P, Gariano SL, Terranova OG (2010) Coupling limit equilibrium analyses and real-time monitoring to refine a landslide surveillance system in Calabria (southern Italy). Nat Hazards Earth Syst Sci 10(11):2341–2354

Jiao JJ, Nandy S (2001) Confined groundwater zone and slope instability in hillsides of weathered igneous rock in Hong Kong. Hong Kong Geol 7:31–37

Jiao JJ, Wang XS, Nandy S (2005) Confined groundwater zone and slope instability in weathered igneous rocks in Hong Kong. Eng Geol 80(1–2):71–92

Leung AK, Ng CWW (2013) Seasonal movements and groundwater flow mechanism in an unsaturated saprolitic hillslope. Landslides 10(4): 455–467

Li C, Ma T, Zhu X, Li W (2011) The power–law relationship between landslide occurrence and rainfall level. Geomorphology 130(3): 221–229

Liang WL, Kosugi K, Mizuyama T (2007) Heterogeneous soil water dynamics around a tree growing on a steep hillslope. Vadose Zone J 6(4):879–889

Ma T, Li C, Lu Z, Bao Q (2015) Rainfall intensity-duration thresholds for the initiation of landslides in Zhejiang Province, southeast China. Geomorphology 245:193–206

Moore ID (1981) Infiltration equations modified for surface effects. J Irrig Drain Div 107(1):71–86

Ng CWW, Menzies B (2007) Advanced unsaturated soil mechanics and engineering. Taylor & Francis, London

Pagano L, Picarelli L, Rianna G, Urciuoli G (2010) A simple numerical procedure for timely prediction of precipitation-induced landslides in unsaturated pyroclastic soils. Landslides 7(3):273–289

Rogers NW, Selby MJ (1980) Mechanisms of shallow translational landsliding during summer rainstorm: North Island, New Zealand. Geogr Ann 62A(1–2):11–21

Smethrust JA, Clarke D, Powrie W (2006) Seasonal changes of pore water pressure in a grass-covered cut slope in London clay. Geotechnique 56(8):523–537

Sun HY, Zhong J, Zhao Y, Shen SJ, Shang YQ (2013) The influence of localized slumping on groundwater seepage and slope stability. J Earth Sci 24(1):104–110

Terzaghi K, Peck RB (1967) Soil mechanics in engineering practice. John Wiley and Sons, New York

National Bureau of Statistics of the People's Republic of China (NBS) (2011) Statistical Yearbook of China. China statistics Press, Beijing (in Chinese)

Tsaparas I, Rahardjo H, Toll DG, Leong EC (2003) Infiltration characteristics of two instrumented residual soil slopes. Can Geotech J 40(5): 1012–1032

Tu XB, Kwong AKL, Dai FC, Tham LG, Min H (2009) Field monitoring of rainfall infiltration in a loess slope and analysis of failure mechanism of rainfall-induced landslides. Eng Geol 105(1–2):134–150

Wieczorek GF (1996) Landslide triggering mechanisms. Landslides: Inv Mitig 247:76–90

Wilson RC (1989) Rainstorms, pore pressures, and debris flows: a theoretical framework. Landslides in a semi-arid environment, 2nd edn. Publications of the Inland Geological Society, California, pp. 101–117

Zhao QL, Sun HY, Wang ZL, Shang YQ (2012) Influence of confined water on translational landslide. Chin J Rock Mech Eng 31(4):762–769 (in Chinese with English abstract)